BJR

https://doi.org/10.1259/bjr.20180568

Received: 27 June 2018 | Revised: 05 October 2018 | Accepted: 24 October 2018

Cite this article as:
Tau N, Berlin A, Yeung I, Halankar J, Murphy G, Jhaveri KS, et al. Quantitative assessment of dynamic ^{18}F-flumethycholine PET and dynamic contrast enhanced MRI in high risk prostate cancer. *Br J Radiol* 2019; **91**: 20180568.

FULL PAPER

Quantitative assessment of dynamic ^{18}F-flumethycholine PET and dynamic contrast enhanced MRI in high risk prostate cancer

[1]NOAM TAU, MD, [2]ALEJANDRO BERLIN, MD, [2]IVAN YEUNG, MSc, PhD, [1]JAYDEEP HALANKAR, MD, [1]GRAINNE MURPHY, MB, BCh, BAO, [1]KARTIK S. JHAVERI, MD, [1]SANGEET GHAI, MD and [1]UR METSER, MD, FRCPC

[1]Joint Department of Medical Imaging, Princess Margaret Hospital, University Health Network, Mount Sinai Hospital and Women's College Hospital, University of Toronto, Toronto, ON, Canada
[2]Department of Radiation Oncology, University of Toronto and Radiation Medicine Program, Princess Margaret Cancer Centre, University Health Network, Toronto, ON, Canada

Address correspondence to: Dr Ur Metser
E-mail: *ur.metser@uhn.ca*

Objective: To describe dynamic ^{18}F-flumethycholine PET (dPET) and dynamic contrast enhancement MR (DCE MR) parameters in localized high-risk prostate cancer (PCa), and determine whether these differ from normal prostate. Furthermore, to determine whether a correlation exists between dPET and DCE MR parameters.
Methods: 41 consenting patients who underwent prostate DCE MR and dPET were included in this institutionally approved study. Intraprostatic lesions on MR were assigned a PI-RADS v2 score, and focal lesions on PET were documented. All lesions were correlated with pathology. Quantitative and semi-quantitative DCE MR and two-tissue compartmental model dPET parameters were determined and tumor-to-normal gland ratios (T/N) for these parameters were calculated. Finally, dPET and DCE MR correlation was estimated using Spearman correlation coefficients.
Results: There were 46 malignant lesions per standard of reference. On dPET, peripheral zone (PZ) tumors had higher K1 ($p < 0.001$), and a T/N ratio ≥2 was significant ($p < 0.001$). On DCE MR, the parameters in, kep, Ktrans and quantitative iAUC were higher for PZ and non-PZ tumors than corresponding normal tissue ($p < 0.001$); for PZ tumors, a T/N ratio ≥ 1.5 for Ktrans and pei was significant ($p = 0.0019$ and 0.0026, respectively). Moderate Spearman correlation ($0.40 < \rho < 0.59$) was found between dPET K1 and DCE MR Ktrans and pei.
Conclusion: In patients with high-risk PCa, quantitative dPET and DCE-MR parameters in primary tumors differ from normal tissue. Only moderate correlation exists between K1 (dPET) and Ktrans and pei (DCE MR). The incremental value of any of these parameters to PI-RADS v2 warrants further investigation.
Advances in knowledge: Unique quantitative and semi-quantitative FCH PET/MR parameters in PCa differ from normal gland, and should be further investigated to determine their potential contribution to PI-RADS v2 in the detection of clinically significant PCa.

INTRODUCTION

Multiparameteric MRI (mpMR) of the prostate gland combining anatomical and functional imaging, including diffusion-weighted imaging (DWI) and dynamic contrast enhancement (DCE MR) has shown value in the detection, localization, risk stratification and staging of clinically significant prostate cancer (PCa).[1,2] The Prostate Imaging Reporting and Data System (PI-RADS) provides a structured reporting system and evidence-based approach to the interpretation of prostate mpMR. DCE MR, commonly interpreted qualitatively has limited added value to mpMR and is considered a complementary, optional sequence in PI-RADS v. 2 (v2).[3,4]

Although PI-RADS v2 performs well in detecting clinically significant PCa, when assessing all category 3–5 lesions, its accuracy is only moderate.[5] A recent study has suggested that qualitative visual assessment of DCE MR may improve the stratification of PI-RADS v2 category 3 (indeterminate) lesions.[6] However, the impact of semi-quantitative or quantitative DCE MR assessment methods in clinical settings has not been well-established.[7,8]

The role of positron emission tomography (PET) in the management of PCa is evolving. In recent years, various radiotracers including ^{18}F-flucholine PET have been evaluated, predominantly in the setting of biochemical recurrence after primary therapy. The basis for choline PET in

PCa is the increase in choline transport and overexpression of choline kinase in tumor cells.[9,10] Only a few studies have assessed the ability of choline PET to detect localized PCa.[11–14] Most authors have used qualitative assessment, with or without semi-quantitative measures, with moderate success. The overlap in radiotracer uptake between benign prostatic abnormalities (*e.g.* prostatitis, adenomatous hyperplasia) and malignancy appears to limit the specificity of choline PET. The performance of quantitative parameters obtained from dynamic PET (dPET) in the detection of PCa is not well-established, and to the best of our knowledge no prior studies have assessed ^{18}F-flumethylcholine (FCH) dPET for this purpose.

The primary objective in the current study was to describe quantitative dPET and DCE MR parameters in patients with high risk PCa, and to determine whether these parameters differ in normal prostate gland. A secondary exploratory aim was to determine whether a correlation exists between quantitative dPET and DCE MR parameters.

METHODS AND MATERIALS

Study design & population

This was a prospective institutionally approved, single-center, single-arm clinical trial evaluating the role of FCH PET/MR for staging high-risk PCa (hrPCa) [NCT#01993160]. The study was designed according to the 2015 guidelines for Standard for Reporting of Diagnostic Accuracy.[15] Consecutive patients with previously untreated, biopsy proven hrPCa were accrued between January 2014 and July 2016. Patients were considered as having hrPCa if histologically proven adenocarcinoma of prostate and one or more of the following criteria were met: Gleason score (GS) ≥8; and/or clinical stage ≥T3a; and/or serum prostate-specific antigen (PSA) >20 ng ml^{-1}. Exclusion criteria included prior therapy for PCa, or contraindication for contrast-enhanced MR. Although the study protocol included prostate and whole-body imaging, the present report focuses on evaluating the role of dPET and DCE MR of the prostate.

Imaging protocol

Patients were scanned on one of two imaging platforms: PET/CT (Siemens Biograph mCT 40, Siemens Healthcare, Knoxville, TN) and 3 T MR (Magnetom Skyra, Siemens Healthcare, Erlangen, Germany), with imaging usually performed on same day (median, 0 d; range, 0–18 d) (n = 31); or integrated PET/MR, when made available in the University Health Network (Biograph mMR, Siemens Healthcare, Erlangen, Germany) (n = 10). All patients received 20 mg of antiperistaltic agent hyoscine butylbromide (Buscopan; Boehringer Ingelheim, Germany) prior to the MR examination.

MR protocol

MRI was acquired in the supine position using a torso phased-array coil placed anteriorly, and spine matrix array coil placed posteriorly. Pulse sequences acquired included sagittal and axial two-dimensional T_2 weighted turbo spin echo, axial two-dimensional diffusion-weighted single-shot echoplanar imaging, variable flip-angle T_1 mapping and DCE MR (Supplementary Table 1). Gadobutrol (Gadovist; Bayer Healthcare, Toronto, ON) was administered at a dose of 0.1 mmol/kg body weight, and at a rate of 2 mL/sec followed by a 30 ml saline flush at 2 ml/s.

PET protocol

Injected dose of FCH was 3.6 MBq/kg body weight (maximum 400 MBq). Pelvic dPET acquisition was obtained immediately after injection using list mode every minute for 10 min.[16–18] For display purposes, list mode frames were divided into 4 frames of 30 s, 4 frames of 60 s and 2 frames of 120 s each. To determine quantitative image derived input curves, list mode frames were also divided into 35 frames (24 frames × 5 s, 6 frames × 30 s, 5 frames × 60 s). A static frame was acquired at a time between 11.3 and 18.9 min, with the majority of patients having the static performed frame at 14 min. The dynamic phase together with the static frame were used for dynamic PET analysis. These were used to estimate arterial blood tracer activity in lieu of invasive blood sampling.[19] In patients who underwent separate MR and PET/CT, unenhanced CT was obtained for scatter and attenuation correction (120 kV, 40–100mA, 5.0 mm reconstructed section thickness, 2.0 mm overlap), and images were corrected for attenuation and reconstructed iteratively with time-of-flight (3 iterations and 21 subsets) using a 256 matrix and a 5 mm gaussian smooth. For patients who underwent integrated PET/MR, MR-based attenuation correction maps were generated from 2-point Dixon gradient-echo sequence in the coronal plane.[20] PET images were corrected for attenuation and reconstructed iteratively (3D OP-OSEM) with 3 iterations and 21 subsets using a 172 matrix and a 4 mm gaussian smooth. Whole body PET acquisition commenced immediately after the dPET.

Demographic and clinical data

Patient age, clinical stage, baseline serum PSA, biopsy-derived GS, sextant location of positive cores on biopsy and surgery (when available) were recorded.

Standard of reference

All lesions were scored according to PI-RADS v2. Patients scanned before the introduction of PI-RADS v2 had a second reading session retrospectively, with an updated PI-RADS v2 score assigned. Correlation of MR- and/or PET-identified lesions was performed to focal and/or systematic biopsies using sextant zonal anatomy, or surgical pathology when available. Given the known difficulty in accurately localizing systematic biopsies to lesions, any biopsy-proven tumor within a sextant or adjacent sextant on same side was considered as having positive pathology.[21] Lesions were considered to be malignant if they were assigned a PI-RADS v2 score of 5 with positive pathology; PI-RADS v2 score ≥3 with spatially consistent positive PET and pathology. Lesions deemed suspicious based on a single modality (either PET or MR) with equivocal or negative biopsy were considered indeterminate and were not analyzed in this study.

Image analysis

All prior imaging and clinical data was available to the readers at time of study interpretation. PET was read by a single fellowship-trained radiologist with 15 years' experience interpreting PET and abdominal imaging (UM). Prostate MR was independently read by one of two fellowship-trained abdominal

Figure 1. Two tissue compartmental model illustration. C_p and C_d are FCH concentration in arterial blood and the diffusive compartment. C_t is the FCH concentration in the tumor compartment. Rate constants k_1, k_2 and k_3 denote the transport in the directions shown. FCH, ^{18}F-flumethylcholine.

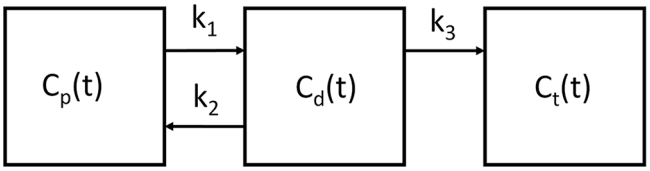

radiologists with 16 years' experience each (SG, KSJ). Dedicated fusion software was used to analyze PET (Thinking Systems MDStation v5.00b; Thinking Systems Corporation, St. Petersburg, FL or Mirada XD3 v3.6.8; Mirada Medical USA, Denver, CO). PET and MR data sets obtained separately were fused on Mirada XD3 v3.6.8 workstation, when needed. MR was reviewed on in-house PACS (Coral Workstation 3.6, University Health Network, Toronto, Canada). All suspicious lesions on MR and PET were grouped according to side and zone (peripheral zone (PZ) or non-PZ (=combining the transition zone, central zone and anterior fibromuscular stroma) and concordance between PET and MR lesions was recorded.

Dynamic PET quantitative analysis

PET images were transferred to a dedicated workstation (ClearCanvas Workstation 2.0, Synaptive Medical, Toronto, Canada), and ROIs were drawn by one of two radiologists (NT, JH) with contour accuracy confirmation by a third independent radiologist (UM).

Dynamic PET data were analyzed with a two-tissue compartment model (Figure 1).[22,23] C_p and C_d are the FCH concentration in arterial blood and the diffusive compartment respectively, while C_t is that in the tumor compartment where Choline is bound. Rate constants k_1, k_2 and k_3 describe the transport as illustrated in Figure 1. Backflux from the tumor to diffusive compartment is ignored for the 10 to 20 min duration of the dynamic study, as FCH is retained within cells in this initial period.[16–18] ROIs drawn on PET images would comprise of all three compartments. Hence, the operating equation can be written as:

$$C_{ROI}(t) = V_p C_p(t) + k_1 \int_0^t e^{-(k_2+k_3)(t-\tau)} C_p(\tau)\, d\tau + \left(\frac{k_1 k_3}{k_2 + k_3}\right) \int_0^t \left[1 - e^{-(k_2+k_3)(t-\tau)}\right] C_p(\tau)\, d\tau$$

where C_{ROI} is FCH concentration over an ROI and V_p is the blood volume. $C_p(t)$ was measured based on the dynamic PET images over an ROI drawn on the external iliac or proximal common femoral artery, with partial volume correction.[24] Detailed derivation of $C_p(t)$ is shown in (Supplementary Material 1). With C_{ROI} and C_p, an in-house non-linear optimization algorithm based on the constrained quasi-Newton method in the NAG library (The Numerical Algorithms Group (NAG), Oxford, United Kingdom) was used to determine the parameters (V_p, k_1, k_2 and k_3). We used only k_1 data in our study, as the main goal was to assess perfusion related parameters.

Figure 2. Peripheral zone dynamic PET K_1 value in the study cohort, comparing values in normal tissue and in tumors. PET, positron emission tomography; PZ, peripheral zone.

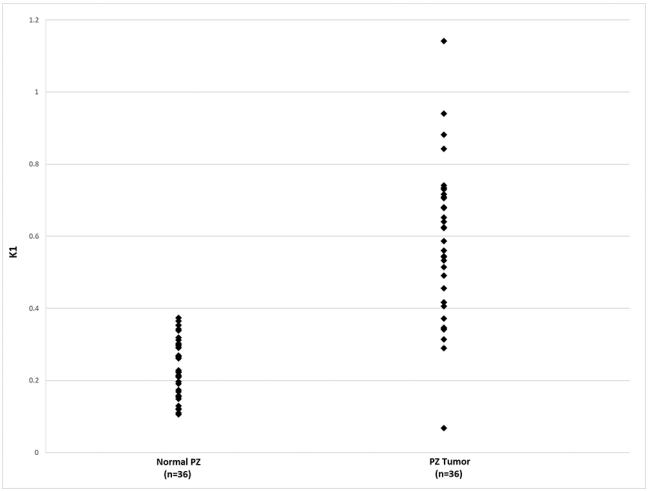

DCE-MR quantitative analysis

MR images were transferred to a Siemens Syngo MR platform, which includes a dedicated module for dynamic analyses of DCE MR (Tissue4D; Siemens Healthcare, Erlangen, Germany). For quantitative analysis of lesions' perfusion parameters, a volume of interest (VOI) was manually drawn on T_2 weighted axial images to cover as much of the tumor volume as possible. If technically feasible, further separate VOIs were drawn to include normal PZ and normal non-PZ. Similar to PET, VOIs were drawn by one of two radiologists with contour accuracy confirmation by a third radiologist. Enhancement kinetics were based on the two-compartmental pharmacokinetic model described by Tofts.[25,26] The arterial input function (AIF) was chosen as "intermediate", the default population averaged options offered by Tissue4D software, to achieve reproducibility across the study population (Figure 2).[27] Semi-quantitative parameters obtained were: washin (*in*); washout (*out*); positive enhancement integral (*pei*); arrival time (*at*); time to peak (*ttp*); and area under the curve (*iAUC*). Quantitative parameters (Tofts model) included: transfer constant from plasma to extracellular extravascular (EES) space (*Ktrans*); volume of EES per unit volume of tissue (*Kep*); flux rate constant between EES and plasma (*Ve*); and *iAUC*.

Data analysis and statistical method

The association between dPET/DCE MR parameters and PCa was examined using paired *t*-test. Tumor to normal background ratios for the quantitative and semi-quantitiatve dPET and DCE MR parameters were determined. Two-sided one sample signed test was used to calculate tumor to normal ratio cut-off significance for PCa. Correlation between dPET and DCE MR parameters was estimated using spearman correlation coefficients. All tests were two-tailed, with $p < 0.05$ considered statistically significant. All analyses were performed using SAS 9.2 (SAS Institute Inc., Cary, NCA) and R 3.0.0 (The R Foundation for Statistical Computing, Vienna, Austria). Further analysis exploring a potential correlation between primary and total GS with the DCE and dPET parameters found to be significant was performed using Microsoft Excel 2016 (Microsoft Corporation, Redmond, WA)

RESULTS

41 consenting patients underwent both DCE MR and dPET of the prostate, and were included in the current analysis (median age, 65 years; range 50–82). Median serum PSA at enrollment and GS were 21.0 ng ml^{-1} (range, 2.99–160 ng ml^{-1}) and 7 (range, 7–9), respectively. One patient had his prostate diffusely replaced by tumor, and no normal tissue could be identified on either dPET or DCE MR dPET data was available for all but three patients, including the aforementioned patient, in which dPET data were corrupt, and normal PZ and normal non-PZ could not be contoured in two and five patients, respectively. Overall, 63 lesions were identified on at least one modality. Each patient had at least one lesion with a PI-RADS v2 score of 4 (10 lesions) or 5 (40 lesions). Furthermore, there were four lesions with PI-RADS v2 score of 3, and nine other lesions that could only be identified on PET with no MR correlate. Of the 63 lesions, 46 were considered as definite tumors according to the standard of reference, of which 39/46 (84.8%) were assigned PI-RADS v2 score of 5; 5/46 (10.9%) were assigned a PI-RADS v2 score of 4 and 2/46 (4.3%) were assigned a PI-RADSv2 score of 3 with concordant PET and sextant histopathology. There were 17/63 lesions (27%) that were deemed indeterminate, of which nine were identified on PET [with equivocal ((n = 5) or negative (n = 4) biopsy); four on MR (with equivocal (n = 2) or negative (n = 2) biopsy)]; and four additional lesions on MR with PI-RADS v2 score of 3 (n = 2) or 4 (n = 2) with no PET correlate and no definitive tumor on biopsy. Indeterminate lesions were not included in the current analysis.

Analysis of dPET and DCE MR parameters for normal prostate and confirmed tumors

For all other patients, dPET (Table 1) and DCE MR (Table 2) parameters for normal prostate and tumors are displayed. Using the prescribed test, differences between the various parameters in normal prostate and tumors were calculated. These were possible only in those patients in which both normal and tumor values could be obtained. In dPET, only *K1* in PZ tumors was significantly higher than normal prostate (Table 3 and Figure 3). For DCE MR, significant differences between PCa and normal tissue were seen in several parameters. In the semi-quantitative analysis, *in* and *iAUC* and in the quantitative analysis, *Ktrans* and *kep* were significantly elevated for both PZ and in non-PZ tumors, and *pei* was significant for PZ tumors, compared to normal tissue (Table 3). Exploratory analysis of correlation between primary and total GS and DCE and dPET parameters shown to be significant revealed considerable overlap between the quantitative parameters and pathologic grade (Figure 4).

Spearman's rank correlation coefficients (ρ) between dPET and DCE MR parameters for tumors was calculated, and is displayed inFigure 5. Moderate correlation ($0.40 > \rho > 0.59$) was found between *K1* and both *Ktrans* and *pei*. Strong correlation ($\rho > 0.60$) could not be found between dPET and DCE MR parameters.

Tumor to normal ratios (T/N) for dPET and DCE MR were calculated for PZ tumors (Table 4). Given the small number of non-PZ tumors in our cohort, alongside lack of normal non-PZ in half of these patients, T/N ratios were not calculated for non-PZ tumors. Using the two-sided one sample signed test, a

Table 1. Distribution of dPET parameters in normal gland and tumors

	Peripheral zone						Non-peripheral zone					
	Normal			Tumor			Normal			Tumor		
Parameter	n	Mean (SD)	Median (Range)	n	Mean (SD)	Median (Range)	n	Mean (SD)	Median (Range)	n	Mean (SD)	Median (Range)
K1 **(ml/min/g)**	36	0.237 (0.081)	0.226 (0.106,0.374)	36	0.58 (0.21)	0.604 (0.068,1.142)	33	0.399 (0.144)	0.404 (0.081,0.762)	7	0.466 (0.238)	0.405 (0.194,0.942)

SD, standard deviation; dPET, dynamic positron emission tomography.

Table 2. Distribution of DCE parameters in normal gland and tumors

	Peripheral zone						Non-peripheral zone					
	Normal			Tumor			Normal			Tumor		
Parameter	*n*	Mean (SD)	Median (Range)	*n*	Mean (SD)	Median (Range)	*n*	Mean (SD)	Median (Range)	n	Mean (SD)	Median (Range)
Quantitative												
Ktrans (min^{-1})	40	0.066 (0.051)	0.048 (0.01,0.241)	38	0.2 (0.178)	0.15 (0.03,0.87)	40	0.108 (0.072)	0.089 (0.02, 0.334)	8	0.182 (0.103)	0.165 (0.055, 0.4)
Kep (min^{-1})	40	0.446 (0.278)	0.378 (0.015,1.32)	38	0.905 (0.658)	0.8 (0.15, 3.52)	40	0.547 (0.277)	0.5 (0.05, 1.15)	8	1.106 (0.541)	1.015 (0.37, 2.18)
Ve ($ml\ g^{-1}$)	40	0.268 (0.197)	0.195 (0.05, 0.995)	38	0.251 (0.114)	0.24 (0.06, 0.531)	40	0.27 (0.145)	0.248 (0.11, 0.975)	8	0.201 (0.132)	0.18 (0.081, 0.51)
iAUC	40	0.828 (1.453)	0.103 (0.005,4.77)	38	3.064 (7.525)	0.205 (0.03,36.05)	40	1.643 (3.105)	0.152 (0.015, 11.065)	8	3.746 (6.667)	0.26 (0.066, 16.77)
Semi-quantitative												
in	40	0.18 (0.122)	0.149 (0.015, 0.533)	38	0.55 (0.432)	0.493 (0.06, 2.24)	40	0.629 (0.355)	0.58 (0.129, 1.25)	8	0.629 (0.355)	0.58 (0.129, 1.25)
o***ut***	40	0.014 (0.014)	0.015 (−0.012, 0.04)	38	0.0038 (0.0842)	0.0015 (−0.21, 0.42)	40	−0.017 (0.045)	−0.02 (−0.1, 0.05)	8	−0.017 (0.045)	−0.02 (−0.1, 0.05)
ttp	40	0.722 (0.338)	0.665 (0.205, 1.615)	38	0.557 (0.345)	0.46 (0.04, 1.99)	40	0.418 (0.097)	0.4 (0.3, 0.61)	8	0.418 (0.097)	0.4 (0.3, 0.61)
at	40	0.725 (0.22)	0.75 (0,1.37)	38	0.744 (0.221)	0.75 (0,1.37)	40	0.796 (0.122)	0.75 (0.65, 1.052)	8	0.796(0.122)	0.75 (0.65, 1.052)
pei	40	0.148 (0.075)	0.126 (0.045,0.4)	38	0.329 (0.176)	0.306 (0.06,0.93)	40	0.298 (0.119)	0.33 (0.101, 0.48)	8	0.298 (0.119)	0.33 (0.101, 0.48)
iAUC2	40	0.084 (0.054)	0.068 (0.015,0.256)	38	0.245 (0.153)	0.215 (0.03,0,73)	40	0.23 (0.104)	0.23 (0.066, 0.38)	8	0.23 (0.104)	0.23 (0.066, 0.38)

DCE, dynamic contrast enhanced ; SD, standard deviation.

Table 3. Differences of dPET and MR DCE parameters between tumor and normal prostate

Parameter	Peripheral zone				Non-peripheral zone			
	N	Mean difference [a]	95% CI	*p* value†	*N*	Mean difference [a]	95% CI	*p* value†
dPET								
K1	35	0.332	0.266,0.398	**<0.001**	4	0.071	−0.078.0.219	0.229
DCE: Quantitative								
ktrans	37	0.418	0.220,0.617	**<0.001**	8	0.083	0.014,0.151	**0.025**
kep	37	0.121	0.070,0.172	**<0.001**	8	0.613	0.285,0.941	**0.003**
ve	37	0.026	−0.028,0.080	0.333	8	−0.169	−0.408,0.070	0.139
iAUC	37	2.371	0.154,4.589	**0.037**	8	2.621	−1.511,6.753	0.177
DCE: Semi-quantitative								
in	37	0.357	0.223,0.490	**<0.001**	8	0.314	0.080,0.549	**0.016**
out	37	−0.009	−0.037,0.018	0.496	8	−0.030	-0.050,−0.010	**0.010**
ttp	37	−0.154	-0.271,−0.037	**0.011**	8	−0.181	−0.398, 0.037	0.090
at	37	0.007	−0.014,0.027	0.513	8	0.087	−0.073, 0.246	0.240
pei	37	0.171	0.114,0.228	**<0.001**	8	0.086	−0.017, 0.189	0.088
iAUC	37	0.154	0.106,0.202	**<0.001**	8	0.096	0.017, 0.176	**0.024**

CI, confidence interval; DCE, dynamic contrast enhancement; dPET, dynamic positron emission tomography.
[a]Mean difference between tumor and normal sample. †Paired *t*-test *p* value.

Figure 3. Spearman's rank correlation heat map between dPET and DCE MR parameters in tumors. DCE, dynamic contrast enhancement; dPET, dynamic positron emission tomography; SUV_{max},maximum standardized uptake value.

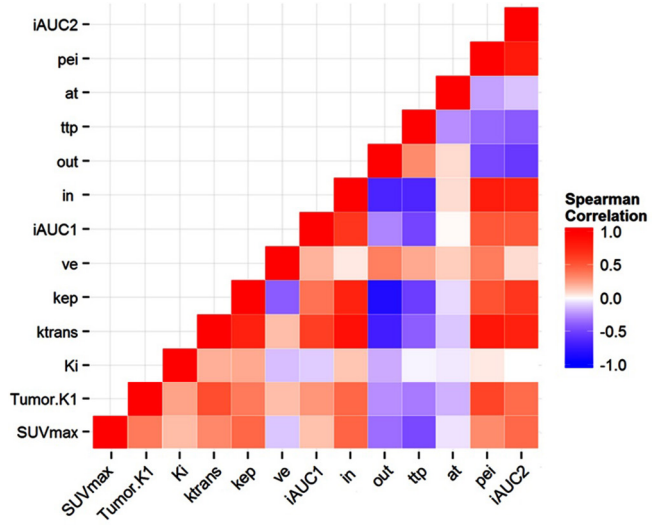

T/N ratio ≥2 for *K1* on dPET was significant ($p < 0.001$). Of the DCE MR parameters, a $T/N \geq 1.5$ for *Ktrans* and *pei* was found to be significant ($p = 0.0019$ and $p = 0.0026$, respectively) and for the semi-quantitative parameter *in* (wash in), a $T/N \geq 2$ showed borderline significance ($p = 0.049$).

DISCUSSION

In patients with PCa, MRI is the imaging modality of choice for local tumor detection and assessment. PI-RADS v2 has reasonable performance in detecting clinically significant PCa. For PI-RADS v2 score ≥4 lesions, the sensitivity and specificity of mpMR for detecting GS ≥7 tumor is 78.9–87.8% and 75.5–79.1%, respectively.[28] Additional parameters, including functional imaging may potentially improve the performance of mpMR. For example, although DCE MR is only a complementary sequence in PI-RADS v2, a recent study has suggested that a modified binary DCE MR score (positive *vs* negative) improves the performance of PI-RADS v2 for detection of transitional zone tumors and the authors suggested using this parameter as an amendment to the PI-RADS two scoring system.[28] In recent years, with the advent of PET/MR, there has been an increased interest in data obtained from both PET and MR to characterize and stage patients with PCa.[29] Data on the clinical utility of quantitative dynamic PET and DCE MR parameters in the detection and characterization of PCa are still limited.

Figure 4. Color-coded *kep* parameter map superimposed on an axial T_2 weighted image of the prostate (Tissue 4D software, Siemens Healthcare). VOI3 is a volume-of-interest drawn on a biopsy proven left peripheral zone GS 9(4+5) tumor. VOI4 was drawn on the contralateral normal right peripheral zone. (B) Quantitative concentration curve and values for the corresponding VOIs. Note that *ktrans,Kep and iAUC* are higher in VOI3 (tumor) compared to VOI4 (normal tissue). GS, Gleason score; VOI, volume of interest.

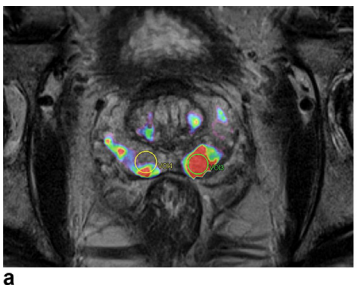

a

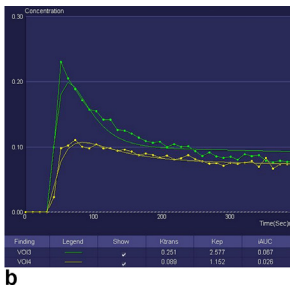

b

The main goal of the current study was to describe the dPET and DCE MR parameters in hrPCa and to determine whether these parameters differ in malignant tumors compared to normal tissue. On dPET, there was significantly higher *K1*, estimating tissue perfusion and choline transport, for PZ tumors as compared to normal gland. On DCE MR, the semi-quantitative parameter *in,* representing contrast washin rate, was significantly different for both PZ and non-PZ tumors; and *pei,* a semi-quantitative parameter which represents the summation of the total signal above baseline, a tissue perfusion parameter[30] was significantly different for PZ tumors. On quantitative DCE MR, *Ktrans* (diffusion of contrast to the extracellular space) and *Kep* (reverse reflux rate constant), were significant for PZ and non-PZ tumors. *Ktrans* may correlate with vascular permeability when blood flow is high compared to permeability or it may correlate with blood flow when permeability is high relative to flow.[31] No strong correlation was found between dPET and DCE MR parameters; therefore, these are not interchangeable nor surrogate of each other. The moderate correlation between *K1* (dPET) and *Ktrans* and *pei* (DCE MR) may be explained by their common dependence on perfusion.

Correction due to metabolite and plasma partitions was not applied to the arterial input in dPET. Prior investigators proposed a correction method by scaling the arterial input by a factor of 1.3 to 1.1 linearly over 0 to 60 min.[32] Although our scan duration was relatively short (up to 20 min), the shape of corrected arterial input curve was found to be almost identical to that of the original curve (not shown here). Therefore, if the correction factor was used, the correct arterial input for this study would have been 1.3 times greater in magnitude. Hence, K1 values in our study are overestimated by up to the same factor (1.3) across the entire cohort as a result of not applying the correction. Such "overestimation" does not affect the correlative and relative comparisons in the cohort. Using the two-tissue compartment model on FCH dPET data of relatively short duration has limitations as discussed in Schaefferkoetter et al.[32] According to their investigation, our K1 values would have a relatively small bias of 8 to 12% due to short duration (up to 11 to 20 min). Therefore, we believe our K1 values are expected to be reasonably accurate within the intrinsic variability of compartmental rate parameter estimates.

The quantitative DCE MR parameters in our cohort differ from prior publications.[32–35] For example, *Ktrans* values in our study were lower than previously reported. Nonetheless, despite the variability in absolute values, the DCE MR parameters identified in the current study as most reliably differentiating PCa

Figure 5. Box-and-whisker plot comparing primary and total GS with the most significant parameters. (a) Correlates GS with *K1* on dPET; (b) compares GS with *ktrans* on DCE MR.Note the significant overlap between all plots. DCE, dynamic contrast enhancement; dPET, dynamic positron emission tomography; GS, Gleasonscore.

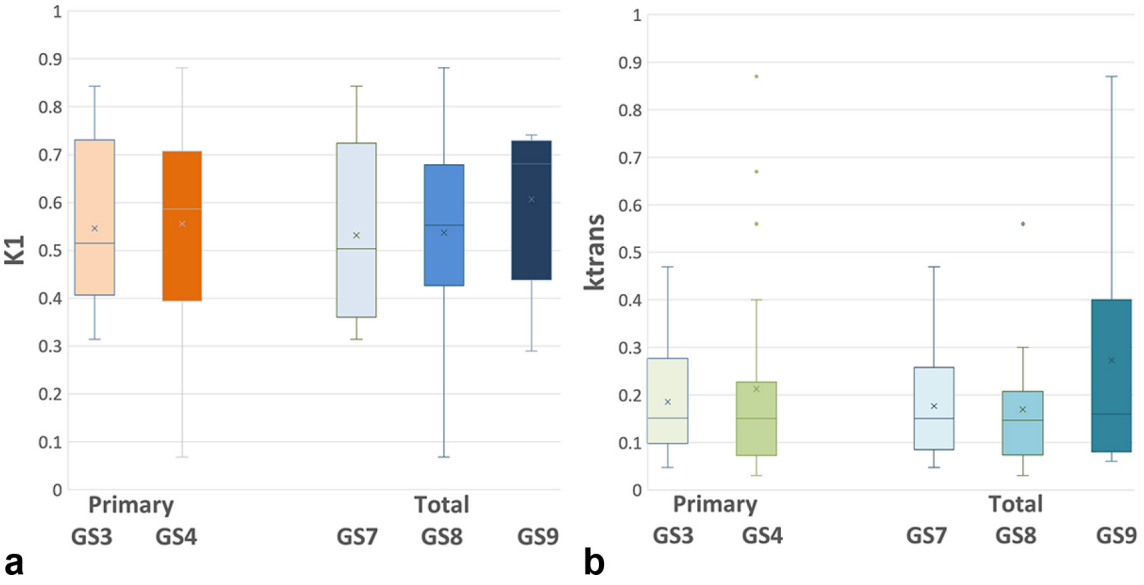

from normal tissue (*in*, *Ktrans*, *Kep*) were in line with previous published studies, including a recent meta-analysis encompassing 484 patients across 14 studies.[7,36] The differences in the absolute values obtained in different studies may be related to a few factors, including differences in software used to analyze DCE MR, choice of AIF and perhaps differences in study population, which in the current study included only patients with hrPCa.[37] From a practical clinical perspective, FCH-dPET can be obtained in the first 10 min after injection ("uptake time") prior to a static whole-body PET. When using integrated PET/MR, the dPET data can be obtained simultaneously with prostate mpMR, without impact on overall scan time. Nonetheless, the results from the current study, including the significance of T/N thresholds obtained for the various parameters need to be validated in independent data sets. Furthermore, it remains to be determined whether incorporating any or all of these quantitative dPET/DCE MR parameters into the diagnostic algorithm of prostate mpMR would improve overall diagnostic accuracy or disease characterization, especially for PI-RADS v2 score 3 and 4 lesions. Moreover, the described quantitative approaches may have further value in the context of increasingly used novel PCa-specific tracers.

Table 4. Distribution of T/N ratios of dPET and DCE parameters for PZ tumor

Parameter	*N*	Mean ratio (SD)	95% Confidence interval
dPET			
K1	35	2.421 (0.869)	2.123–2.72
DCE: Quantitative			
ktrans	35	3.65 (4.784)	2.007–5.294
kep	35	2.231 (2.003)	1.543–2.919
ve	37	1.44 (0.916)	1.134–1.745
iAUC	37	3.355 (3.742)	2.107–4.603
DCE: Semi-quantitative			
in	37	4.194 (4.265)	2.772–5.616
out	35	1.061 (5.905)	−0.967–3.09
ttp	37	0.837 (0.4)	0.704–0.97
at	36	1.012 (0.084)	0.984–1.041
pei	37	2.418 (1.575)	1.893–2.943
iAUC	37	3.674 (2.929)	2.697–4.651

DCE, dynamic contrast enhancement; SD, standard deviation; dPET, dynamic positron emission tomography.

Our study has a few limitations. First, the study population included patients with hrPCa and the quantitative results may only be applicable to this cohort. Second, we did not have targeted lesion biopsies or whole mount pathology for many of the presumed tumors. However, we have used the previously described method of sextant confirmation ("Rosenkrantz method") for PI-RADS four or five lesions.[21] Third, we defined lesions with PI-RADS score of 4 as indeterminate unless pathologically confirmed, as defined by the standard of reference. Although this may have resulted in the exclusion of some tumors, we believe this is justifiable given the limited positive-predictive value of PI-RADS four lesions, noted to be up to 64%.[21,38] Fourth, we did not evaluate benign prostate lesions, such a focal prostatitis, to determine whether any of the significant quantitative parameters identified would contribute to the specificity of FCH PET/MR. This would need to be evaluated in future studies. Finally, our method of analysis of dPET and DCE MR may have varied from other researchers and this may have resulted in different absolute values for some of the described parameters. We attempted to broaden the applicability of our method by evaluating T/N ratios with significant cutoffs found for *K1* on dPET and *Ktrans* and *pei* on DCE MR.

CONCLUSION

In conclusion, in patients with hrPCa, unique quantitative and semi-quantitative FCH PET/MR parameters in primary tumors differ from those obtained in normal tissue. Only a moderate correlation exists between *K1* on dPET and *Ktrans* on DCE MR The incremental value of any or all of these parameters in the detection of clinically significant PCa to the existing PI-RADS v2 interpretation criteria warrants further investigation.

FUNDING

This work was awarded by Prostate Cancer Canada and is proudly funded by the Movember Foundation – Grant # D2013-28.

PATIENT CONSENT

This was a prospective institutionally approved study, and all patients have signed an informed consent form [NCT#01993160]

REFERENCES

1. Fütterer JJ, Briganti A, De Visschere P, Emberton M, Giannarini G, Kirkham A, et al. Can Clinically Significant Prostate Cancer Be Detected with Multiparametric Magnetic Resonance Imaging? A Systematic Review of the Literature. *Eur Urol* 2015; **68**: 1045–53. doi: https://doi.org/10.1016/j.eururo.2015.01.013
2. Simmons LAM, Kanthabalan A, Arya M, Briggs T, Barratt D, Charman SC, et al. The PICTURE study: diagnostic accuracy of multiparametric MRI in men requiring a repeat prostate biopsy. *Br J Cancer* 2017; **116**: 1159–65. doi: https://doi.org/10.1038/bjc.2017.57
3. Vargas HA, Hötker AM, Goldman DA, Moskowitz CS, Gondo T, Matsumoto K, et al. Updated prostate imaging reporting and data system (PIRADS v2) recommendations for the detection of clinically significant prostate cancer using multiparametric MRI: critical evaluation using whole-mount pathology as standard of reference. *Eur Radiol* 2016; **26**: 1606–12. doi: https://doi.org/10.1007/s00330-015-4015-6
4. De Visschere P, Lumen N, Ost P, Decaestecker K, Pattyn E, Villeirs G. Dynamic contrast-enhanced imaging has limited added value over T2-weighted imaging and diffusion-weighted imaging when using PI-RADSv2 for diagnosis of clinically significant prostate cancer in patients with elevated PSA. *Clin Radiol* 2017; **72**: 23–32. doi: https://doi.org/10.1016/j.crad.2016.09.011
5. Kim SH, Choi MS, Kim MJ, Kim YH, Cho SH. Validation of prostate imaging reporting and data system version 2 using an MRI-ultrasound fusion biopsy in prostate cancer diagnosis. *AJR Am J Roentgenol* 2017; **209**: 800–5. doi: https://doi.org/10.2214/AJR.16.17629
6. Druskin SC, Ward R, Purysko AS, Young A, Tosoian JJ, Ghabili K, et al. Dynamic contrast enhanced magnetic resonance imaging improves classification of prostate lesions: A study of pathological outcomes on targeted prostate biopsy. *J Urol* 2017; **198**: 1301–8. doi: https://doi.org/10.1016/j.juro.2017.07.011
7. Gao P, Shi C, Zhao L, Zhou Q, Luo L. Differential diagnosis of prostate cancer and noncancerous tissue in the peripheral zone and central gland using the quantitative parameters of DCE-MRI: a meta-analysis. *Medicine* 2016; **95**: e5715. doi: https://doi.org/10.1097/MD.0000000000005715
8. Vos EK, Litjens GJ, Kobus T, Hambrock T, Hulsbergen-van de Kaa CA, Barentsz JO, et al. Assessment of prostate cancer aggressiveness using dynamic contrast-enhanced magnetic resonance imaging at 3 T. *Eur Urol* 2013; **64**: 448–55. doi: https://doi.org/10.1016/j.eururo.2013.05.045
9. Ramírez de Molina A, Rodríguez-González A, Gutiérrez R, Martínez-Piñeiro L, Sánchez J, Bonilla F, et al. Overexpression of choline kinase is a frequent feature in human tumor-derived cell lines and in lung, prostate, and colorectal human cancers. *Biochem Biophys Res Commun* 2002; **296**: 580–3. doi: https://doi.org/10.1016/S0006-291X(02)00920-8
10. Sutinen E, Nurmi M, Roivainen A, Varpula M, Tolvanen T, Lehikoinen P, et al. Kinetics of [(11)C]choline uptake in prostate cancer: a PET study. *Eur J Nucl Med Mol Imaging* 2004; **31**: 317–24. doi: https://doi.org/10.1007/s00259-003-1377-9
11. Hara T, Kosaka N, Kishi H. PET imaging of prostate cancer using carbon-11-choline. *J Nucl Med* 1998; **39**: 990–5.
12. Hara T, Kosaka N, Kishi H. Development of (18)F-fluoroethylcholine for cancer imaging with PET: synthesis, biochemistry, and prostate cancer imaging. *J Nucl Med* 2002; **43**: 187–99.
13. Beheshti M, Imamovic L, Broinger G, Vali R, Waldenberger P, Stoiber F, et al. 18F choline PET/CT in the preoperative staging of prostate cancer in patients with intermediate or high risk of extracapsular disease: a prospective study of 130 patients. *Radiology* 2010; **254**: 925–33. doi: https://doi.org/10.1148/radiol.09090413
14. Schmid DT, John H, Zweifel R, Cservenyak T, Westera G, Goerres GW, et al. Fluorocholine PET/CT in patients with prostate cancer: initial experience. *Radiology* 2005; **235**: 623–8. doi: https://doi.org/10.1148/radiol.2352040494
15. Bossuyt PM, Reitsma JB, Bruns DE, Gatsonis CA, Glasziou PP, Irwig L, et al. STARD 2015: an updated list of essential items for reporting diagnostic accuracy studies. *Radiology* 2015; **277**: 826–32. doi: https://doi.org/10.1148/radiol.2015151516
16. DeGrado TR, Coleman RE, Wang S, Baldwin SW, Orr MD, Robertson CN, et al. Synthesis and evaluation of 18F-labeled choline as an oncologic tracer for positron emission tomography: initial findings in prostate cancer. *Cancer Res* 2001; **61**: 110–7.
17. DeGrado TR, Reiman RE, Price DT, Wang S, Coleman RE. Pharmacokinetics and radiation dosimetry of 18F-fluorocholine. *J Nucl Med* 2002; **43**: 92–6.
18. DeGrado TR, Baldwin SW, Wang S, Orr MD, Liao RP, Friedman HS, et al. Synthesis and evaluation of (18)F-labeled choline analogs as oncologic PET tracers. *J Nucl Med* 2001; **42**: 1805–14.
19. Verwer EE, Oprea-Lager DE, van den Eertwegh AJ, van Moorselaar RJ, Windhorst AD, Schwarte LA, et al. Quantification of 18F-fluorocholine kinetics in patients with prostate cancer. *J Nucl Med* 2015; **56**: 365–71. doi: https://doi.org/10.2967/jnumed.114.148007
20. Delso G, Fürst S, Jakoby B, Ladebeck R, Ganter C, Nekolla SG, et al. Performance measurements of the Siemens mMR integrated whole-body PET/MR scanner. *J Nucl Med* 2011; **52**: 1914–22. doi: https://doi.org/10.2967/jnumed.111.092726
21. Rosenkrantz AB, Ginocchio LA, Cornfeld D, Froemming AT, Gupta RT, Turkbey B, et al. Interobserver reproducibility of the PI-RADS version 2 lexicon: A multicenter study of six experienced prostate radiologists. *Radiology* 2016; **280**: 793–804. doi: https://doi.org/10.1148/radiol.2016152542

22. Casciari JJ, Graham MM, Rasey JS. A modeling approach for quantifying tumor hypoxia with [F-18]fluoromisonidazole PET time-activity data. *Med Phys* 1995; **22**: 1127–39. doi: https://doi.org/10.1118/1.597506
23. Gunn RN, Gunn SR, Cunningham VJ. Positron emission tomography compartmental models. *J Cereb Blood Flow Metab* 2001; **21**: 635–52. doi: https://doi.org/10.1097/00004647-200106000-00002
24. Metran-Nascente C, Yeung I, Vines DC, Metser U, Dhani NC, Green D, et al. Measurement of tumor hypoxia in patients with advanced pancreatic cancer based on 18F-fluoroazomyin arabinoside uptake. *J Nucl Med* 2016; **57**: 361–6. doi: https://doi.org/10.2967/jnumed.115.167650
25. Tofts PS, Kermode AG. Measurement of the blood-brain barrier permeability and leakage space using dynamic MR imaging. 1. Fundamental concepts. *Magn Reson Med* 1991; **17**: 357–67. doi: https://doi.org/10.1002/mrm.1910170208
26. Tofts PS, Brix G, Buckley DL, Evelhoch JL, Henderson E, Knopp MV, et al. Estimating kinetic parameters from dynamic contrast-enhanced T(1)-weighted MRI of a diffusable tracer: standardized quantities and symbols. *J Magn Reson Imaging* 1999; **10**: 223–32. doi: https://doi.org/10.1002/(SICI)1522-2586(199909)10:3<223::AID-JMRI2>3.0.CO;2-S
27. Orton MR, d'Arcy JA, Walker-Samuel S, Hawkes DJ, Atkinson D, Collins DJ, et al. Computationally efficient vascular input function models for quantitative kinetic modelling using DCE-MRI. *Phys Med Biol* 2008; **53**: 1225–39. doi: https://doi.org/10.1088/0031-9155/53/5/005
28. Rosenkrantz AB, Babb JS, Taneja SS, Ream JM. Proposed adjustments to PI-RADS version 2 decision rules: Impact on prostate cancer detection. *Radiology* 2017; **283**: 119–29. doi: https://doi.org/10.1148/radiol.2016161124
29. Choi JY, Yang J, Noworolski SM, Behr S, Chang AJ, Simko JP, et al. ^{18}F Fluorocholine dynamic time-of-flight PET/MR imaging in patients with newly diagnosed intermediate- to high-risk prostate cancer: initial clinical-pathologic comparisons. *Radiology* 2017; **282**: 429–36. doi: https://doi.org/10.1148/radiol.2016160220
30. Nadrljanski M, Maksimović R, Plešinac-Karapandžić V, Nikitović M, Marković-Vasiljković B, Milošević Z. Positive enhancement integral values in dynamic contrast enhanced magnetic resonance imaging of breast carcinoma: ductal carcinoma in situ vs. invasive ductal carcinoma. *Eur J Radiol* 2014; **83**: 1363–7. doi: https://doi.org/10.1016/j.ejrad.2014.05.006
31. Verma S, Turkbey B, Muradyan N, Rajesh A, Cornud F, Haider MA, et al. Overview of dynamic contrast-enhanced MRI in prostate cancer diagnosis and management. *AJR Am J Roentgenol* 2012; **198**: 1277–88. doi: https://doi.org/10.2214/AJR.12.8510
32. Schaefferkoetter JD, Wang Z, Stephenson MC, Roy S, Conti M, Eriksson L, et al. Quantitative ^{18}F-fluorocholine positron emission tomography for prostate cancer: correlation between kinetic parameters and Gleason scoring. *EJNMMI Res* 2017; **7**: 25. doi: https://doi.org/10.1186/s13550-017-0269-0
33. Sanz-Requena R, Martí-Bonmatí L, Pérez-Martínez R, García-Martí G. Dynamic contrast-enhanced case-control analysis in 3T MRI of prostate cancer can help to characterize tumor aggressiveness. *Eur J Radiol* 2016; **85**: 2119–26. doi: https://doi.org/10.1016/j.ejrad.2016.09.022
34. Langer DL, van der Kwast TH, Evans AJ, Plotkin A, Trachtenberg J, Wilson BC, et al. Prostate tissue composition and MR measurements: investigating the relationships between ADC, T2, K(trans), v(e), and corresponding histologic features. *Radiology* 2010; **255**: 485–94. doi: https://doi.org/10.1148/radiol.10091343
35. Ocak I, Bernardo M, Metzger G, Barrett T, Pinto P, Albert PS, et al. Dynamic contrast-enhanced MRI of prostate cancer at 3 T: a study of pharmacokinetic parameters. *American Journal of Roentgenology* 2007; **189**: W192–W201. doi: https://doi.org/10.2214/AJR.06.1329
36. Kim SH, Choi MS, Kim MJ, Kim YH, Cho SH. Role of semi-quantitative dynamic contrast-enhanced MR imaging in characterization and grading of prostate cancer. *Eur J Radiol* 2017; **94**: 154–9. doi: https://doi.org/10.1016/j.ejrad.2017.06.021
37. Othman AE, Falkner F, Kessler DE, Martirosian P, Weiss J, Kruck S, et al. Comparison of different population-averaged arterial-input-functions in dynamic contrast-enhanced MRI of the prostate: Effects on pharmacokinetic parameters and their diagnostic performance. *Magn Reson Imaging* 2016; **34**: 496–501. doi: https://doi.org/10.1016/j.mri.2015.12.009
38. Chen F, Cen S, Palmer S. Application of prostate imaging reporting and data system version 2 (PI-RADS v2): interobserver agreement and positive predictive value for localization of intermediate- and high-grade prostate cancers on multiparametric magnetic resonance imaging. *Acad Radiol* 2017; **24**: 1101–6. doi: https://doi.org/10.1016/j.acra.2017.03.019